Simulation annealing diagnosis algorithm method for optimized forecast of the dynamic response of floating offshore wind turbines

Peng Chen [1], Lei Song [2], Jiahao Chen[3], Zhiqiang Hu [1, 4]
1. *School of Engineering, Newcastle University, Newcastle upon Tyne, NE1 7RU, United Kingdom*
2. *School of Naval Architecture and Ocean Engineering, Huazhong University of Science and Technology, Wuhan,430074, China*
3. *Guangdong Electric Power Design Institute Co., Ltd., China Energy Engineering Group, Guangzhou, 510663, China*
4. *College of Shipbuilding Engineering, Harbin Engineering University, Harbin, 150001, China*

Abstract: Design of floating offshore wind turbines (FOWTs) needs reliable and innovative technologies to overcome the challenges on how to better predict the dynamic responses in terms of aero-hydro-servo-elastic disciplines. This paper aims to demonstrate the optimized prediction of the dynamic response of FOWTs by Simulation annealing diagnosis algorithm (SADA). SADA is an Artificial Intelligence technology-based method, which utilizes the advantages of numerical simulation, basin experiment and machine learning algorithms. The actor network in deep deterministic policy gradient (DDPG) is adopted to take actions to adjust the KDPs in each loop according to the feedback of 6DOF motions of platform in dynamic response analysis. The results demonstrated that the mean values of the platform's motions and rotor axial thrust force could be predicted with higher accuracy. On this basis, other physical quantities that designers are more concerned about but cannot be obtained from experiments and actual measurements will be predicted by SADA with more credibility. This SADA method differs from traditional supervised learning applications in renewable energy, which do not need to be provided physical quantities with strong direct correlation. All targets can be artificially set for SADA to obtain a better self-learning performance. In general, designers can use SADA to get a more accurate and optimized prediction of the dynamic response of FOWTs, especially those physical quantities that cannot be directly obtained through the basin experiments.

Key words: Floating offshore wind turbine, SADA, AI-based *DARwind*, Artificial intelligence, Basin experiment.

Introduction

The conception of FOWTs can be traced back to the 1970s, and the first commercialization in the world was in the UK in 2017. Some innovative design of FOWTs also have been proposed and validated. For example, Hywind and DeepCwind in the OC projects[1-4] and OO-Star Wind Floater[5], Nautilus steel semisubmersible[6], IDEOL concrete floater[7] in LIFES50+ project, etc. However, from the conception to the real commercialization, although the FOWTs have been existing for nearly half a century, it still faces many challenges. The challenges are involved particularly prominently from the beginning of the design and operational safety issues [8]. The dynamic model of FOWTs encompasses many engineering disciplines, including: the coupling between aerodynamics loads (turbine) and hydrodynamics loads (floater and mooring lines), flexible structural components (turbine and floater), elasticity, blade pitch controls and restoring effect of the mooring lines, which are all needed to validate their technical and economic feasibility.

Many scholars have summarized some challenges in terms of numerical simulation[9] or experimental validation[10-11]. In addition, some representative basin experimental techniques have been explored including a methodology for the scaling problems by redesigned model scale rotor[12]. Some other specific techniques are concluded, which can be found in reference [13]. Regardless of the scale ratio problem, the physical quantities obtained through experiments are far from meeting the demand of designers. For commercial FOWTs, the business community is more concerned about the response of the superstructure and mooring system. Therefore, it is very important to obtain accurate dynamic responses, which cannot be obtained directly from basin experiments during the design stage. These must rely on a reliable numerical-experimental method or actual measurement.

With development of AI technology, the wind industry gains a lot of creative ideas from its utility and simplicity. Some scholars have reviewed the machine learning application in wind industry in condition monitoring[14] and power forecasting[15]. Similarly, innovations based on offshore platforms or wave energy collectors have also been carried out. For example, the SVM regression model[16] and artificial neural network (ANN)[17], which were developed for the real-time short-term forecast of wave elevations and wave excitation forces. Although the AI technology has greatly promoted the development of the traditional wind power industry and offshore engineering, its applications in FOWTs are still very few. And most of the applications are based on supervised learning,

Biography: Peng Chen (1993-), Male, Master,
E-mail: p.chen8@ncl.ac.uk

Corresponding author: Lei Song, Male, Master,
E-mail: song_lei@hust.edu.cn

relying on a large amount of full-scale data for training and analysis. The predicted physical quantities have certain limitations and must have very strong correlations with the input data. In addition, due to the confidentiality and commercial nature of the full-scale data, it is not easily accessible for most scholars.

Using supervised learning algorithm can directly predict the motion of the FOWTs platform [18], but this also leads to the lack of prediction of other physical quantities, such as the deformation of blades and towers, which are more concerned by the wind industry. Because the experimental physical quantities (EPQs) that can be obtained from experiment are very limited. Designers and industry are also very concerned about those physical quantities (NON-EPQs) that cannot be directly obtained. Therefore, how to obtain these NON-EPQs on basis of EPQs has become another challenge for FOWTs design. An innovative AI-based method[13], named SADA has been proposed, and it can be used to analyze and predict dynamic responses of FOWTs, especially those NON-EPQs. This paper addresses a study on demonstrating the feasibility of SADA method in application of AI-numerical-experimental techniques.

1. Methodology of SADA

The methodology of SADA method is briefly introduced here, including the concept of KDPs and the *DARwind*. The Key Disciplinary Parameters (KDPs) is the first critical concept and tool proposed in SADA method. The second critical tool is *DARwind*, an in-house programme[19], which was developed to conduct dynamic analysis for FOWTs based on fundamental theories. The details of SADA can be referred to reference[13].

1.1 *Key Disciplinary Parameters selection*

The dynamic responses prediction of FOWTs involves multiple disciplines, including aerodynamics, hydrodynamics, structural mechanics, multi-body dynamics and kinematics, mooring dynamics, etc. Many of the functions and formulas involved in these theories are determined based on assumptions and empirical parameter values. However, these empirical parameters values may not be proper for FOWTs due to its high nonlinear coupling effect. Therefore, as the first step of using SADA method, it is of great importance to select these key discipline parameters properly, because critical KDPs will not only bring more accurate calculation results, but also be used as the data exchanging portal during the AI training process in SADA method. Table 1 shows some example KDPs used in this paper.

Table 1 Selected KDPs in SADA

Discipline	KDPs
Aero	Wind speed
	Glauert correction
Hydro	Current speed
	Added linear restoring matrix
	Added linear viscous damping matrix
	Added quadratic viscous damping matrix
	Added static force
Mooring	Wet density
	Axial stiffness
Structural	Polynomial Flap 1st vibration modes
Servo	Generator torque constant

1.2 *AI-based DARwind*

In SADA method, *DARwind* will be trained to be intelligent specially for the objective FOWTs to run the dynamics response analysis with the initial critical KDPs. For more information of the *DARwind* programme, please refer to the published literature[19]. *DARwind* is embedded an AI module. The specific notations and nouns combined FOWTs and Reinforcement Learning (RL) in SADA are:

Agent: *DARwind*
State(S): The numerical results from *DARwind*.
Action(A): Change the KDPs.
Reward(R): The reward and punishment obtained by error assessment.

The Deep Deterministic Policy Gradient (DDPG) algorithm[20] was adopted in AI module to use deep neural networks to estimate the optimal policy function instead of choosing the action based on a specific distribution. The overall layout of SADA combines AI-based *DARwind* and KDPs is presented in Figure 1.

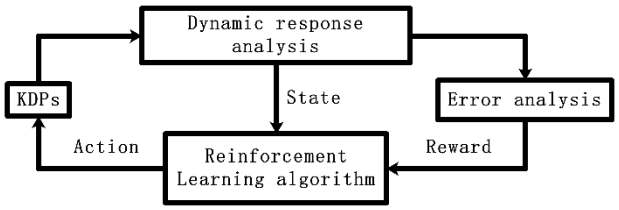

Fig. 1 The overall layout of SADA method.

2. Data collection and Error definition

This section mainly introduces the data collection and error definition in SADA method. The data of the basin experiment will be used as the target data carry out the error assessment. In addition, the [state, action, next state, reward] will be used to train the deep neural network in reinforcement learning algorithm.

2.1 Basin experiment

The model test was carried out at Deepwater Offshore Basin in Shanghai Jiao Tong University with a model set-up corresponding to a 1:50 Froude scaling. Figure 2 shows the experimental model and sensors the 5MW Spar-type floater. More details on the test executions, such as the model blades fabrication, wind field tests, restoring tests of the mooring system can be found in references[21].

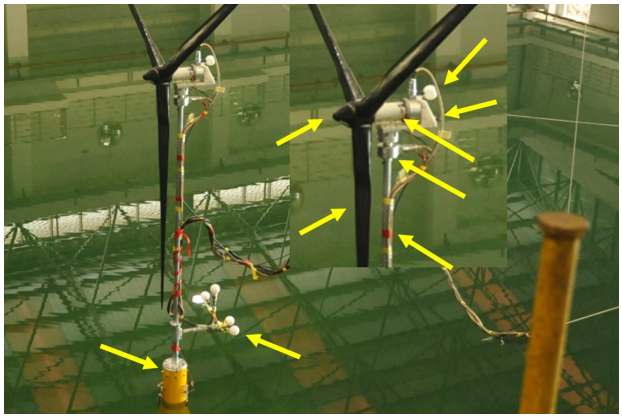

Fig. 2 Experimental model and sensors.

2.2 Case setting

A total of 12 experimental cases were selected for verification, which are shown in Table 2. These cases include the wind only, wave only, current only, wind and wave, wind and wave and current (WWC). The first 9 groups are used by Discrete models in SADA for analysis, so that the numerical simulation results under a single working condition can obtain higher accuracy. The 6^{th} group will be used by Continuous model to predict the unknow cases which are assumed that they have not been carried out in the basin experiment.

In Table 2, the irregular wave is based on the JONSWAP wave spectrum, wherein H_s represents the significant wave height, T_p represents the spectral peak wave period, and γ represents the spectral peak parameter. V_w and V_c are the speed of wind, rotor and current, respectively.

Table 2 Training cases matrix

No		V_w	Wave			V_c
		m/s	H_s (m)	T_p (s)	γ	m/s
1a	current only	-	-	-	-	0.3
1b		-	-	-	-	0.85
2a	wind only	9.4	-	-	-	-
2b		10.9	-	-	-	-
3a	wave only	-	2	8	3.3	-
3b		-	7.1	12.3	2.2	-
4a	wind and current	11.1	-	-	-	0.85
4b		10.9	-	-	-	1.2
5a	wind and wave	12.8	7.1	12.1	2.2	-
5b		10.9	7.1	12.1	2.2	-
6a	WWC	8	2	8	3.3	0.6
6b		11.4	7.1	12.1	2.2	0.8
6c		18	7.1	12.1	2.2	0.85

2.3 Dataset collection

The data is classified according to different cases. Figure 3 briefly illustrates the process of data collection. As the first step of the simulation, the program will perform the first initial calculation, and then perform fitting weights (actions) on KDPs, to obtain the second calculation results and rewards. At this point, [state, action, next state, reward] is stored as a set of training data.

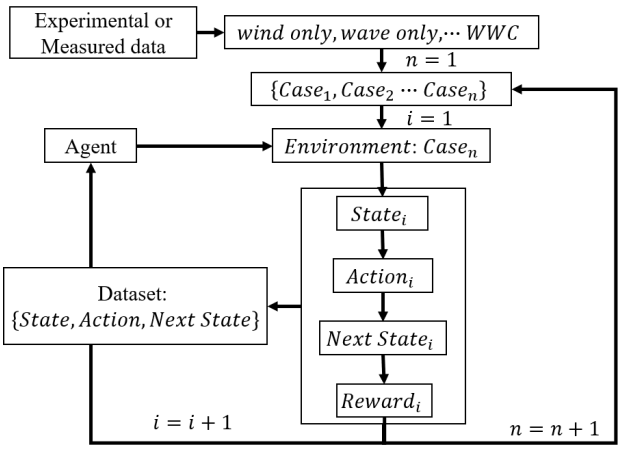

Fig. 3 Data classification and collection

2.4 Error definition

In the study at this moment, only the mean value is considered as the target value for each platform DOF motion. The variation of error ($Error_{\text{variation}}$) is defined as:

$$E_{\text{inital}} = \left| \frac{O_{\text{model test}} - O_{\text{inital KDPs}}}{O_{\text{model test}}} \right| \times 100\% \quad (1)$$

$$E_{\text{present}} = \left| \frac{O_{\text{model test}} - O_{\text{weighted KDPs}}}{O_{\text{model test}}} \right| \times 100\% \quad (2)$$

$$Error_{\text{variation}} = E_{\text{inital}} - E_{\text{present}} \quad (3)$$

The $O_{\text{model test}}$ is the output experimental physical quantity. The $O_{\text{initial KDPs}}$ is the numerical results by initial KDPs by *DARwind*. $O_{\text{weighted KDPs}}$ is the AI training results by weighted KDPs by *DARwind*. The $Error_{\text{variation}}$ is used to measure whether the results of SADA is better than the initial KDPs. If the $Error_{\text{variation}}$ is positive, it means that the error between experiment and numerical simulation has decreased by SADA, otherwise the error has increased.

3. Optimization results by SADA

In this section, the training outcome of SADA method will be demonstrated. Through the error assessment assisted by experimental data, the value network is trained to help *DARwind* to adjust KDPs intelligently according to the feedback of environment. This section will focus on three aspects, which are single impact, two sea loads impact and fully wind/wave/current. The impact here refers to the factors affecting the FOWTs system. The wind only, wave only and current only will be considered in single impact (case 1-3). Wind and wave, wind and current will be considered in coupling impact (case 4-5).

3.1 Single impact

A single impact mainly includes current only (case 1 a & b), wind only (case 2 a & b) and wave only (case 3 a & b) cases in Table 2. Figure 4 summarizes

the results of 6 DOF motions of these 6 cases. The stacked histogram represents the percentage of error change, while the dotted line chart corresponding to the right axis represents the change in amplitude under the corresponding percentage.

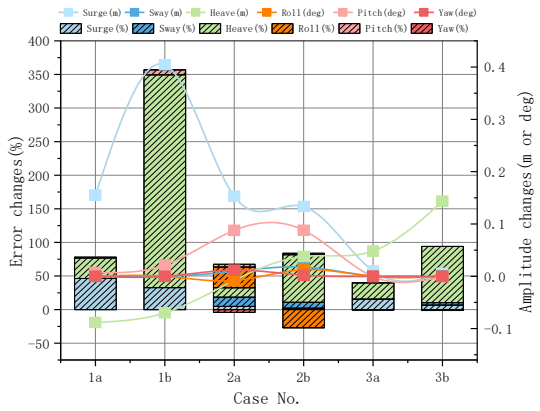

Fig. 4 6DOF motions Error variation in single impact cases.

In current only (case 1 a & b) cases, the current speed has a dominant influence on the FOWTs system. Except for surge motion, the amplitudes of other motions are quite small. The error reductions of surge are 46.35% and 32.68%, and the amplitude of the changes are between 0.16m and 0.4m. Figure 5 shows the time history of surge in 1b. The left coordinate compares the experimental results and simulation results. The right coordinate shows the results of AI-based *DARwind*.

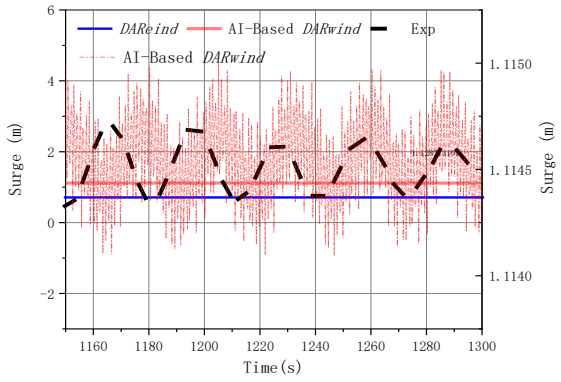

Fig.5 Time history of surge in case 1b

In wind only cases (case 2 a & b), the error percentage of roll has increased, but its experimental amplitude does not exceed 0.03 deg. Taking case 2b as an example, the amplitude changed 0.01 deg. Although this may not be the global optimal solution, it is acceptable for the entire highly coupled FOWTs system. Figure 6 shows the time history of surge and sway in 2b. The amplitude of the surge in 2b changed 0.13m (from 5.52m to 5.65m). The tension error of the fairleads at the connection of the three mooring lines are also reduced by 1.2%, 1.69% and 1.73% (respectively 29.66kN, 49.73kN and 50.83kN).

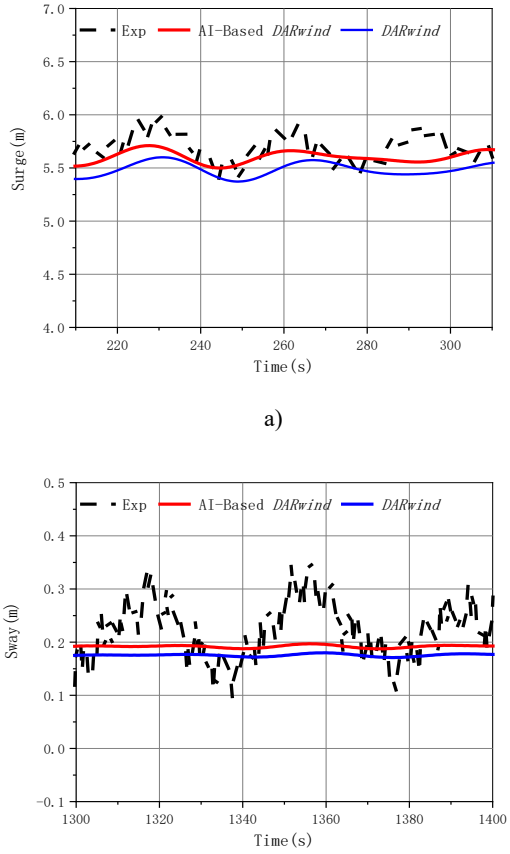

Fig. 6 Time history of surge and sway in case 2b

In the case of wave only (case 3 a & b), the platform is basically maintained in a stable state and the wind turbine is in a shutdown state. Under this environment, heave and pitch motions are the dominating motions. Taking 3b as an example, the mean error of heave has been reduced by 83.71%, which is a very satisfactory optimization result in amplitude. Figure 7 shows the frequency analysis in 3b. From the frequency domain, it can also better show the motion induced by natural frequency of the platform has been improved by SADA.

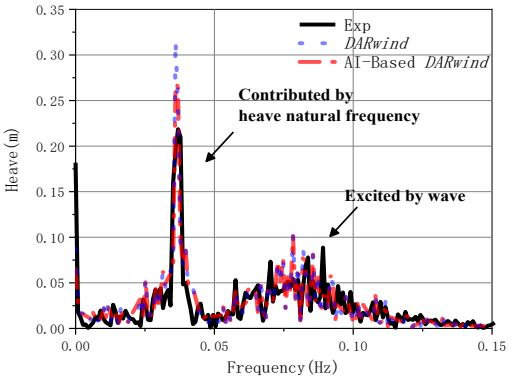

Fig.7 Frequency of heave in case 3b.

Figure 8 shows the change of heave motion in a random 60 explorations. The mooring system plays a vital role in maintaining the stability of the platform in the waves. Since the boundary conditions of KDPs are determined initially based on empirical values, their characteristics can be further analyzed according to the correlation during the training process. More accurate boundary conditions not only change with different environments, but also accelerate the convergence of the model.

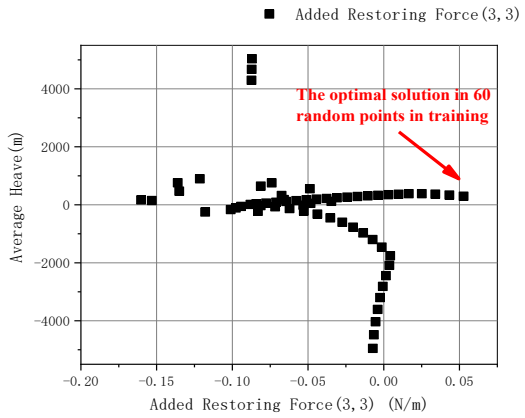

Fig.8 Heave and added restoring force (3,3) in case 3b.

3.2 Two sea loads impact

In this section, The SADA method will be used to verify the optimization of the FOWTs system by the two sea loads, including wind & current cases (case 4 a & b) and wind & wave cases (case 5 a & b). The optimization effect of the six degrees of freedom and the amplitude of the corresponding change are shown in Figure 9. Take case 4b as an example, through the optimization of the SADA method, the mean error of surge is reduced from 3.7% to 0.8%. Figure 10 shows the corresponding time history curve of surge. Although the mean error of Heave has increased by 10%, it is still a relatively ideal change from the perspective of the change in the time history curve (Figure 11).

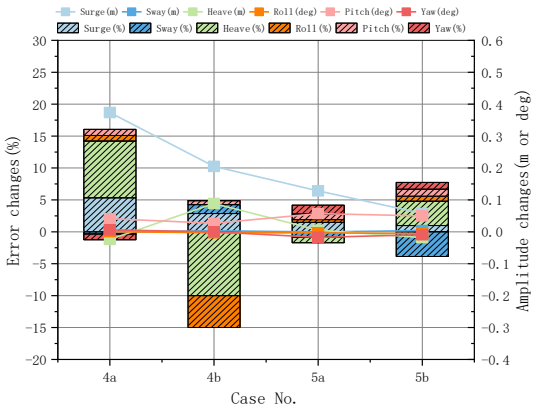

Fig.9 6DOF motion Error variation in two sea loads impact cases.

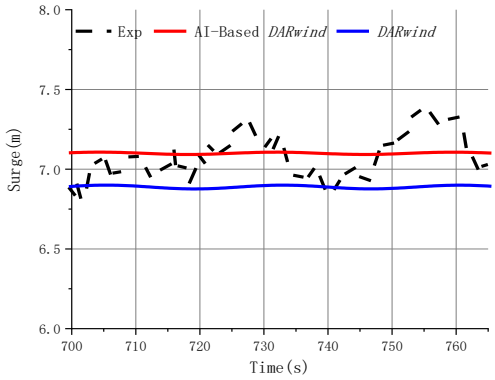

Fig.10 Time history of surge in case 4b

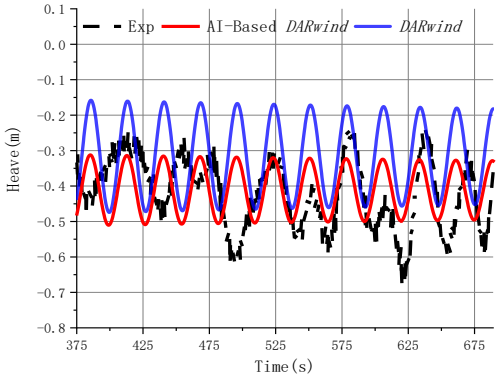

Fig.11 Time history of Heave in case 4b

The coupling of wind and wave will inhibit some motion of the platform. Therefore, in the case of wind and waves, the motions of platform have no obvious amplitude except for surge and pitch.

For basin experiments and numerical simulations, the optimization of single impact is the most challenging. Because based on numerical assumptions,

apart from a single factor, other parts will not affect the entire system. However, this is not the case in actual basin experiments. Even the amplitude of the motion is small, it is more affected by the environment and instruments. In contrast, coupled conditions can indeed better reflect the dynamic response of FOWTs in the actual sea state. In general, the SADA performed well in both single impact and two sea loads impact optimization.

3.3 Wind/wave/current impact

This section will use SADA to optimize the dynamic response of FOWTs in a wind/wave/current sea environment (case 6 a, b and c). Case 6b will be adopted to train the Continuous model in SADA. The duration of the experimental data for Case 6b is 1 hour, and it will be divided into four segments and each contains 900-second target data for training. The axial thrust of the rotor is the most important response that affects the motions of the FOWTs, especially on the pitch motion. For basin experiments, a more matched thrust is the best choice to better simulate the dynamic responses of the FOWTs. However, if the rotor speed and wind speed in the experiment are fully used in the numerical simulation, the thrust force calculated by the numerical value will be different from the measured value, due to the unmatching of low Reynolds number. Therefore, rotor speed is also added to the adjustable KDPs to better simulate the axial thrust of FOWTs in this section.

Figure 12 shows the final error and amplitude change of the four segments. The error between surge and pitch increases slightly. Taking pitch as an example, the error range of the four segments are all within 5 percent. This is a tolerable category in training. The actual amplitude changes are also within the range of 0.2deg.

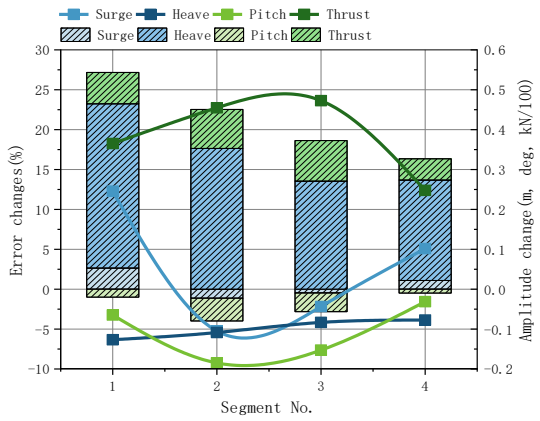

Fig.12 Error and amplitude change of four segments in case 6a.

The error of heave and axial thrust has dropped significantly. Taking the third segment as an example, the average value of thrust has increased by 47.5kN. Figure 13 also shows the thrust increased by 36.5kN. They are all much closer to experimental value. In addition, the mean value of each segment changed significantly from the initial KDPs through SADA. Taking the first segment as an example, the mean error of surge is reduced by 2.6%. The time history curve of pitch and thrust optimized by SADA is closer to the experimental data.

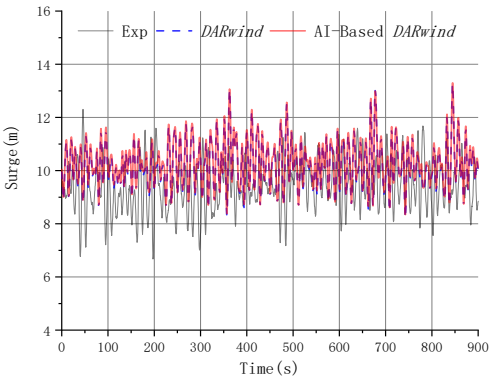

a)

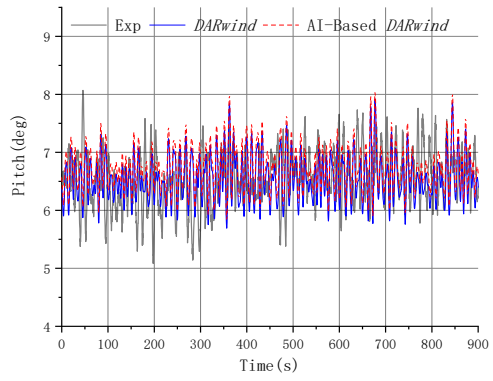

b)

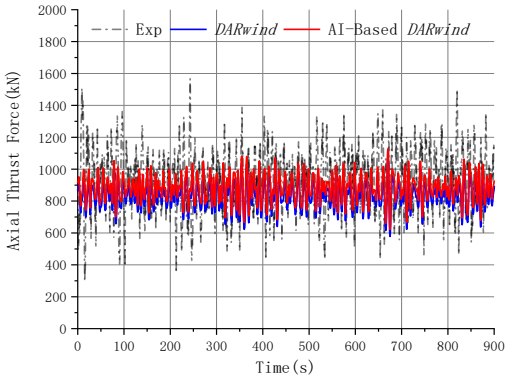

c)

Fig. 13 Time history of surge, pitch and thrust in first segments in case 6b.

It is difficult to see the changes and training conditions of each segment only from the time history curve, so it is necessary to analyze the error changes

during the training, which first requires the classification of the random segment data. Figure 14 shows the variation of the error between surge and pitch in 500 iterations. The 4 color curves represent the error changes of each segment in 500 iterations. It can be seen in the first 20 training sessions, the second group is randomly selected, and then the experimental mean is automatically selected as the fourth group, and so on.

In the first and fourth segmented training (red and purple lines) of surge, the error has a gradually decreasing trend, which is also the same as the final optimization result in Figure 12. The pitch error is stable within a range, although each segment has a small increase. Therefore, to better explore the performance of pitch in 500 iterations, its statistics are listed in Table 4.

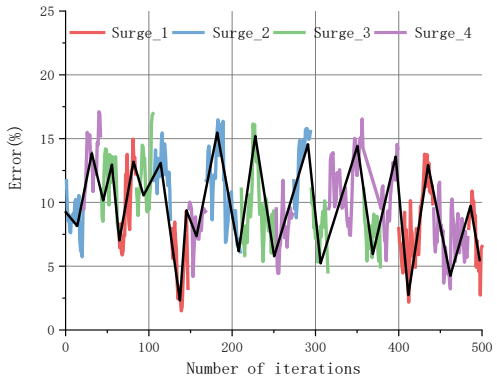

a)

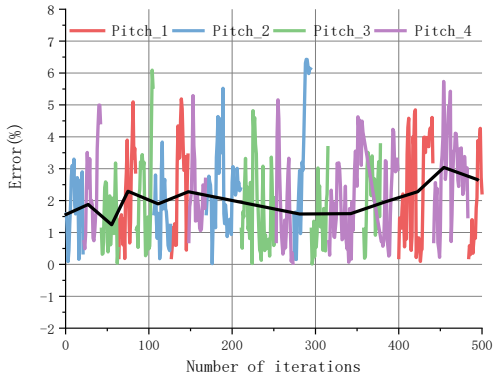

b)

Fig.14 The error of surge & pitch in 500 iterations.

Table 4 Statistical description for Pitch and KDPs

	Avg	SD	Min	Max
Pitch	6.49	0.174	6.19	6.90
Wind	11.35	0.233	11	11.8
Rotor	14.42	0.016	14.48	14.35
Current	0.80	0.080	0.7	0.9

The average pitch values of the four segments are 6.54 deg, 6.42 deg, 6.45 deg and 6.57 deg respectively. The mean value of 500 iterations of numerical simulation is very close to the experimental value. The average value of other KDPs is also consistent with the initial setting of this working condition. The standard deviations of rotor speed and current speed as well as the wet density of the mooring system are very close to zero. This is due to the boundary conditions of these three physical quantities, which are not allowed to change too much. From the maximum and minimum points of view, the wind speed, the rotation speed of the rotor, the axial stiffness of mooring system and the current speed have been cut off after touching the boundary conditions. The wet weight of the mooring system is always within the boundary conditions.

The wind speed not only has a greater impact on the aerodynamic load of FOWTs, but also affects the thrust. Because the blade pitch control is not considered in the experiment, the entire rotor is more sensitive to changes in wind speed. It is a very common simulation technology to adjust the measured wind speed value in numerical simulation so that the axial thrust of the rotor matches the measured value as much as possible. Finally, SADA increased the wind speed to satisfy the thrust similarity as much as possible, although at the expense of some pitch accuracy. This also reflects the weighting effect on the main physical quantities in training. Therefore, it is important for the designers to have a good understanding basic theories and practical technology of FOWTs.

4 Prediction

In this section, the deep neural network model trained in 6b will be applied to predict the cases 6a and 6c. It is assumed that case 6 a & b have not been carried out in the basin experiment, so there is no target value in the error assessment, and the model is only used for weighting the feedback of each loop. There are 10 iterations of forecast optimization.

Figure 15 illustrates that the mean error and amplitude change of the four EPQs (surge, heave, pitch and thrust) in 6b and 6c. in 6b, the mean error of heave decreased by 35.4%. The most significant is the change in thrust, an increase of 51.8kN. The performance of 6c was the best, and the mean error all decreased. This may be because case 6b and 6c have the same wave environment.

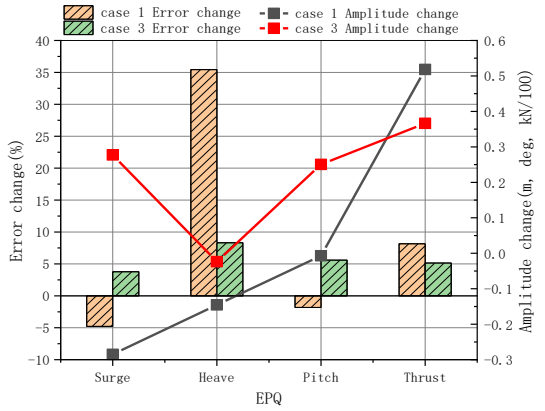

Fig. 15 Error and amplitude change of prediction in 6a and 6c.

Through the forecast of SADA, the thrust in 6a can match better. As shown in Figure 16, the thrust change is quite significant, and although the error of surge and pitch has decreased, it is still acceptable. The pitch curve can be found that the mean error has increased, but the trend of increase is closer to the experimental result. This also shows that the SADA method is not independent from the scope of traditional FOWTs numerical calculations. It must work together with a reliable dynamic response agent, such as *DARwind*, that allows SADA to make judgments and learning faster, more effectively, and more accurately. This is the character that SADA method differs from traditional reinforcement learning methods.

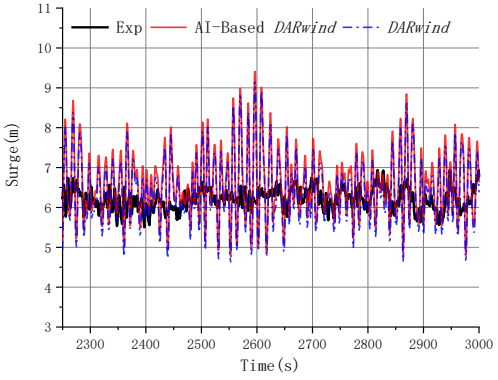

a)

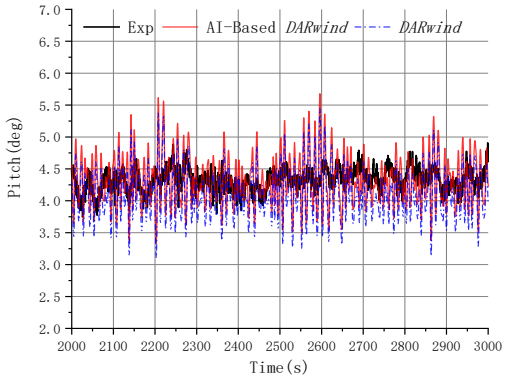

b)

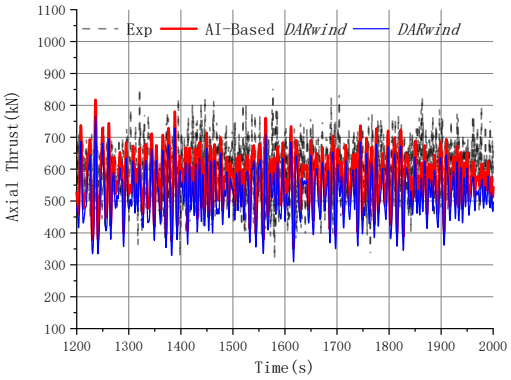

c)

Fig 16. Time history of surge, pitch and thrust in 6a

For the result of 6c, it is not difficult to see from Figure 17 that the error of the mean value of pitch and thrust is reduced through the optimized forecast of SADA. In the numerical simulation, the KDPs corresponding to this result, especially the wind speed and the rotation speed of the rotor, did not reach the boundary conditions. According to the set error weighting, SADA chooses equalization optimization instead of sacrificing the accuracy of some other physical quantities in 6a and 6b.

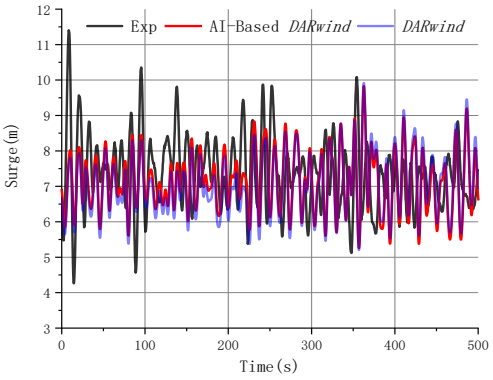

a)

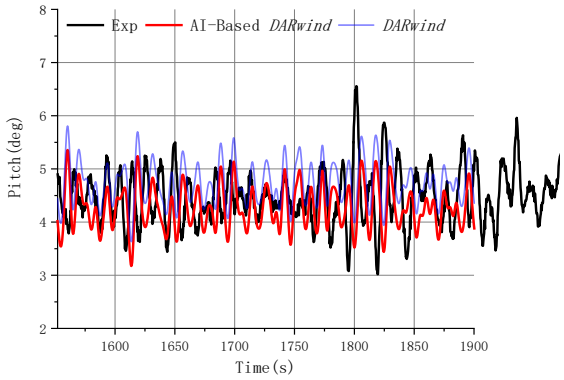

b)

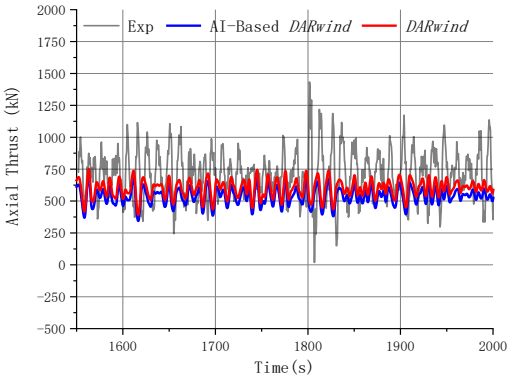

c)

Fig 17. Time history of surge, pitch and thrust in case 6c

SADA optimizes the average of some EPQs to make predictions of NON-EPQs with higher accuracy, such as the deformation of blades and towers. Based on the forecast results in the previous section, some of the optimized NON-EPQs has been shown in Figures 18, including the deformation of the blade tip and tower in two directions.

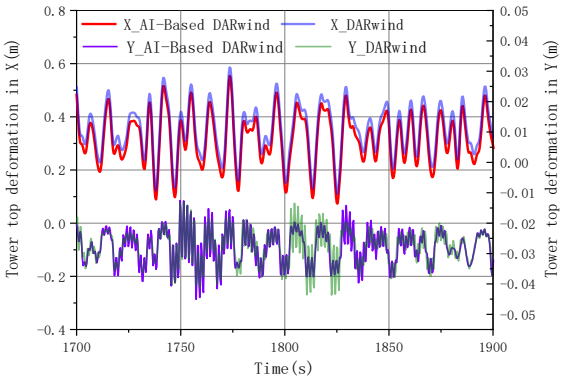

a)

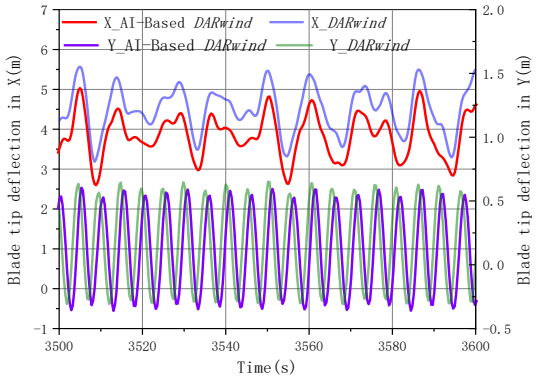

b)

Fig.18 Time history of tower and blade tip deformation under case 6a.

5. Conclusion

The SADA method in this paper combines traditional FOWTs numerical simulation and Artificial Intelligence technology methodology. Two models (discrete and continuous) can be optimized for the different needs of designers. With the accumulation of training data and for different coupling environments, its forecasting effect will be accurate and fast. In the numerical calculation part, not only can the traditional empirical parameters be intelligently adjusted, but also other types of KDPs can be fitted. For the part of artificial intelligence, different from traditional reinforcement learning method, the AI-Based *DARwind*, as an executor of dynamic response simulation, already has a certain degree of credibility and judgment. It is undeniable that the more efficient and accurate the agent, the more credible the training effect of SADA.

However, the SADA method still faces many challenges. It is not only the dependence on the agent, but apart from the hyperparameters of the deep neural network, whether it is the weighting of errors, the setting of boundary conditions for each KDPs, or the restrictions for each action, etc. It takes time and experience to further exploration.

Acknowledgement

The authors acknowledge the State Key Laboratory of Coastal and Offshore Engineering, Dalian University of Technology for funding through grant LP20V4.

References

[1] Jonkman, J., & Musial, W. (2010). Offshore code comparison collaboration (OC3) for IEA Wind Task 23 offshore wind technology and deployment. National Renewable Energy Lab.(NREL), Golden, CO (United States).

[2] Robertson, A., Jonkman, J., Masciola, M., Song, H., Goupee, A., Coulling, A., et al. (2014). Definition of the semisubmersible floating system for phase II of OC4. National Renewable Energy

Lab.(NREL), Golden, CO (United States).
[3] Robertson, A. N., Wendt, F., Jonkman, J. M., Popko, W., Dagher, H., Gueydon, S., et al. (2017). OC5 project phase II: validation of global loads of the DeepCwind floating semisubmersible wind turbine. *Energy Procedia, 137*, 38-57.
[4] Robertson, A. N., Gueydon, S., Bachynski, E., Wang, L., Jonkman, J., Alarcón, D., et al. OC6 Phase I: Investigating the underprediction of low-frequency hydrodynamic loads and responses of a floating wind turbine. In *Journal of Physics: Conference Series, 2020* (Vol. 1618, pp. 032033, Vol. 3): IOP Publishing
[5] Pegalajar-Jurado, A., Bredmose, H., Borg, M., Straume, J. G., Landbø, T., Andersen, H. S., et al. State-of-the-art model for the LIFES50+ OO-Star Wind Floater Semi 10MW floating wind turbine. In *Journal of Physics: Conference Series, 2018* (Vol. 1104, pp. 012024, Vol. 1): IOP Publishing
[6] Galván, J., Sánchez-Lara, M., Mendikoa, I., Pérez-Morán, G., Nava, V., & Rodríguez-Arias, R. NAUTILUS-DTU10 MW Floating Offshore Wind Turbine at Gulf of Maine: Public numerical models of an actively ballasted semisubmersible. In *Journal of Physics: Conference Series, 2018*: Institute of Physics Publishing
[7] Beyer, F., Choisnet, T., Kretschmer, M., & Cheng, P. W. (June 21 2015). Coupled MBS-CFD simulation of the IDEOL floating offshore wind turbine foundation compared to wave tank model test data. In *The Twenty-fifth International Ocean and Polar Engineering Conference, Kona, Hawaii, USA, 2015* (pp. ISOPE-I-15-272)
[8] Zhang, Y., Hu, Z., Ng, C., Jia, C., & Jiang, Z. (2020). Dynamic responses analysis of a 5 MW spar-type floating wind turbine under accidental ship-impact scenario. *Marine Structures, 75*, 102885.
[9] Liu, Y., Li, S., Yi, Q., & Chen, D. (2016). Developments in semi-submersible floating foundations supporting wind turbines: A comprehensive review. *Renewable and Sustainable Energy Reviews, 60*, 433-449, doi:https://doi.org/10.1016/j.rser.2016.01.109.
[10] Chen, P., Chen, J., & Hu, Z. (2020). Review of Experimental-Numerical Methodologies and Challenges for Floating Offshore Wind Turbines. *Journal of Marine Science and Application, 19*(3), 339-361, doi:10.1007/s11804-020-00165-z.
[11] Stewart, G., & Muskulus, M. (2016). A Review and Comparison of Floating Offshore Wind Turbine Model Experiments. *Energy Procedia, 94*, 227-231, doi:https://doi.org/10.1016/j.egypro.2016.09.228.
[12] Müller, K., Sandner, F., Bredmose, H., Azcona, J., Manjock, A., & Pereira, R. (2014). *Improved tank test procedures for scaled floating offshore wind turbines.* Paper presented at the International Wind Engineering Conference, Hannover, Germany
[13] Chen, P., Chen, J., & Hu, Z. (2021). Software-in-the-Loop Combined Reinforcement Learning Method for Dynamic Response Analysis of FOWTs. [Original Research]. *Frontiers in Marine Sciense, 7*(1242), doi:10.3389/fmars.2020.628225.
[14] Stetco, A., Dinmohammadi, F., Zhao, X., Robu, V., Flynn, D., Barnes, M., et al. (2019). Machine learning methods for wind turbine condition monitoring: A review. *Renewable Energy, 133*, 620-635.
[15] Khan, N. M., Khan, G. M., & Matthews, P. AI Based Real-Time Signal Reconstruction for Wind Farm with SCADA Sensor Failure. In *IFIP International Conference on Artificial Intelligence Applications and Innovations, 2020* (pp. 207-218): Springer
[16] Ma, Y. (2020). *Machine learning in ocean applications: wave prediction for advanced controls of renewable energy and modeling nonlinear viscous hydrodynamics*. Ph. D. Thesis, Massachusetts Institute of Technology, Ph. D. Thesis.
[17] Li, L., Gao, Y., Ning, D., & Yuan, Z. (2020). Development of a constraint non-causal wave energy control algorithm based on artificial intelligence. *Renewable Sustainable Energy Reviews*, 110519.
[18] Chen, P., Hu, Z., & Hu, C. (2019). *Software-In-the-Loop Method to Predict the Global Dynamic Responses of Full-scale Floating Wind Turbines by Artificial Neural Network.* Paper presented at the 11th International Workshop on Ship and Marine Hydrodynamics, Hamburg, Germany,
[19] Chen, J., Hu, Z., Liu, G., & Wan, D. (2019). Coupled aero-hydro-servo-elastic methods for floating wind turbines. *Renewable Energy, 130*, 139-153.
[20] Lillicrap, T. P., Hunt, J. J., Pritzel, A., Heess, N., Erez, T., Tassa, Y., et al. (2015). Continuous control with deep reinforcement learning. *Computing Research Repository, abs/1509.02971*.
[21] Duan, F., Hu, Z., & Niedzwecki, J. (2016). Model test investigation of a spar floating wind turbine. *Marine Structures, 49*, 76-96.